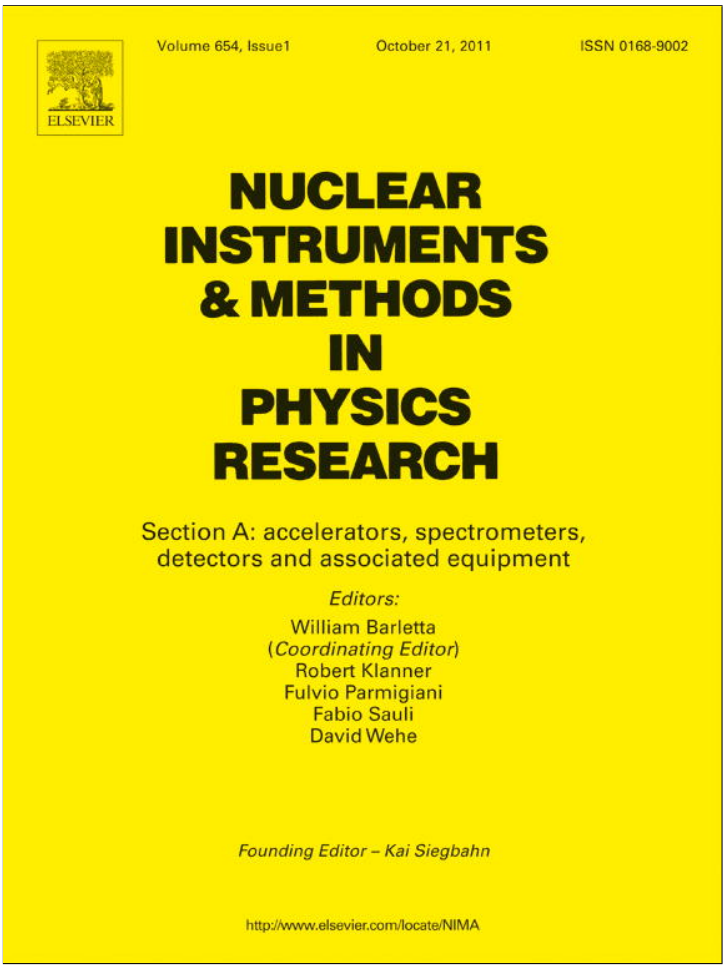

Nuclear Instruments and Methods in Physics Research A 654 (2011) 63–71

Contents lists available at ScienceDirect

Nuclear Instruments and Methods in Physics Research A

journal homepage: www.elsevier.com/locate/nima

The IFMIF-EVEDA challenges in beam dynamics and their treatment

P.A.P. Nghiem [a,*], N. Chauvin [a], M. Comunian [b], O. Delferrière [a], R. Duperrier [a], A. Mosnier [a], C. Oliver [c], D. Uriot [a]

[a] CEA/DSM/IRFU, Centre de Saclay, 91191 Gif-sur-Yvette Cedex, France
[b] INFN/LNL, Legnaro (PD), Italy
[c] CIEMAT, Madrid, Spain

ARTICLE INFO

Article history:
Received 24 January 2011
Received in revised form
15 June 2011
Accepted 22 June 2011
Available online 8 July 2011

Keywords:
Linear accelerator
Beam dynamics
High intensity beam
High power accelerator
High space charge

ABSTRACT

One major system of the IFMIF project (International Fusion Materials Irradiation Facility) is its two accelerators producing the neutron flux by accelerating deuteron particles up to 40 MeV against a lithium target. In the first phase called EVEDA (Engineering Validation and Engineering Design Activity), a full scale prototype accelerating particles up to 9 MeV is being studied and constructed in Europe, to be installed in Japan.

Two unprecedented performances are required for the IFMIF-EVEDA accelerators: very high power of 5 MW and very high intensity of 125 mA CW. This leads to numerous unprecedented challenges in beam dynamics design and optimisation: harmful losses even for those less than 10^{-6} of the beam, non-linear dynamics induced by very strong space charge forces, difficulties for equipment and diagnostic implementations in the high compact structure, need of specific tuning strategies in this context.

These issues are highlighted in this article, and the ways in which they are addressed are detailed.

1. Introduction

The IFMIF project (International Fusion Materials Irradiation Facility) is set in the context of the Fusion Broader Approach signed between Japan and Europe aiming at studying materials, which must resist to very intense neutron radiations in future fusion reactors. One objective is to construct the world's most intense neutron source capable of producing 10^{17} neutrons/s at 14 MeV. A major system of this project is its two accelerators producing the neutron flux by accelerating deuteron particles up to 40 MeV against a lithium target. In the first phase called EVEDA (Engineering Validation and Engineering Design Activity), a full scale prototype accelerating particles up to 9 MeV is being studied and constructed in Europe, to be installed in Japan.

To produce the neutron flux equivalent to those of future fusion reactors, the required deuteron intensity in the accelerators is very high, 125 mA CW, which, combined with the required final energy, makes IFMIF-EVEDA the accelerators of the megawatt class at relatively low energy. This article points out how the simultaneous combination of very high intensity and very high power induces unprecedented challenges for beam dynamic design and optimisation, but also provides exciting opportunities for HIB studies.

2. IFMIF main features

The general layouts of the IFMIF-EVEDA accelerators are displayed in Fig. 1. In each of the two IFMIF accelerators, D^+ particles are first accelerated by the source extraction system, then by the long RFQ and finally the SRF-Linac composed of four cryomodules. The LEBT and MEBT have to focus and match the beam in the 6D phase space from an accelerating structure to another. The HEBT drives the beam to the lithium target where, with the help of multipolar magnetic elements, the transverse beam density must be made flat in a well defined rectangle shape. The EVEDA accelerator is composed of exactly the same sections up to the first cryomodule and a simplified HEBT, which must properly expands the beam toward the beam dump.

Fig. 1 also indicates the beam energies together with beam powers along the accelerators. Due to the very high beam intensity of 125 mA, the beam power is already 625 kW at the RFQ exit and 1.1 MW after the first cryomodule, to reach 5 MW after the 4th cryomodule and that too at relatively low energies of 5, 9 and 40 MeV, where space charge effects are still dominant.

This situation is unique when compared to worldwide linear accelerators in operation or as planned. Fig. 2 shows the average beam power as a function of beam energy for the most powerful accelerators, while Fig. 3 gives for the same accelerators the generalised perveance K, relevant for judging space-charge forces

$$K = qI/2\pi\varepsilon_0 m_0 \gamma^3 v^3 \quad (1)$$

* Corresponding author. Tel.: +33 169089264; fax: +33 169089283.
E-mail address: phu-anh-phi.nghiem@cea.fr (P.A.P. Nghiem).

0168-9002/$ - see front matter © 2011 Elsevier B.V. All rights reserved.
doi:10.1016/j.nima.2011.06.102

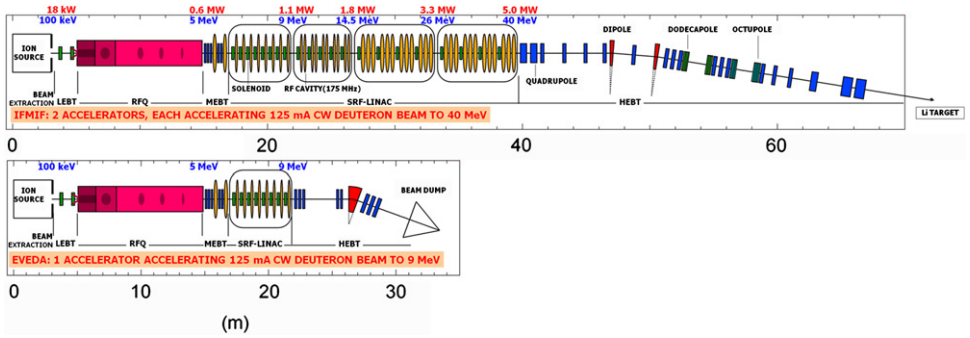

Fig. 1. Layouts of the IFMIF-EVEDA accelerators.

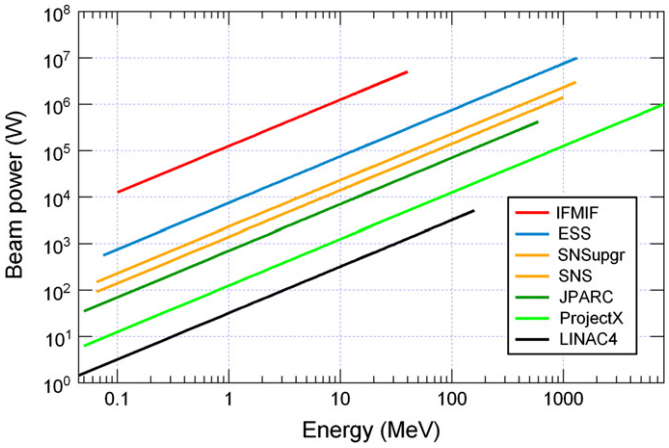

Fig. 2. Average beam power as functions of energy.

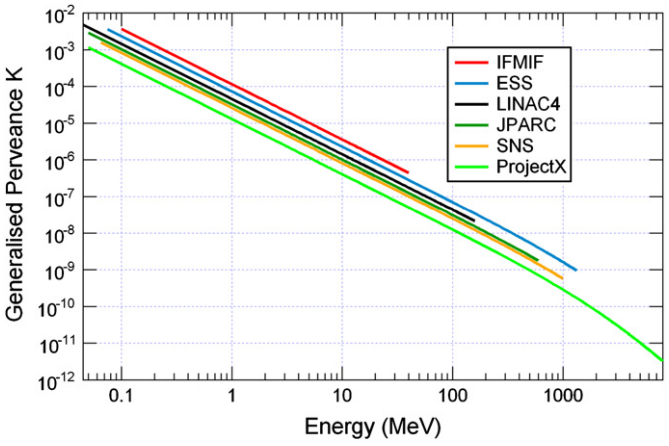

Fig. 3. Generalised perveance as functions of energy.

ε_0 being the vacuum permittivity, I the beam intensity, γ the relativistic factor and m_0, q, v are the particle rest mass, charge and speed, respectively.

In addition to IFMIF are carried forward the proton linacs ESS (Lund, Sweden), Linac4 (CERN, Switzerland), JPARC (Tokai, Japan), SNS (ORNL, USA), ProjectX (FNL, USA). Heavy-ion machines are not displayed because they cannot be easily compared to proton machines. It is nevertheless worth mentioning that high intensity linacs accelerating heavy ions such as FRIB (MSU, USA) for its planned operation with proton comparable to JPARC, and NDCX-II (LNNL, USA) ,which although has a less than 1 W average power, features huge peak power of hundreds MW.

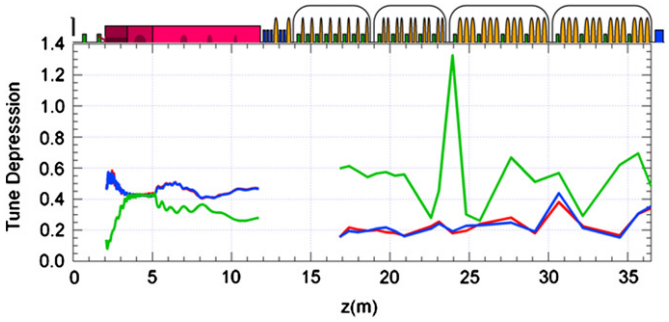

Fig. 4. Tune depression in the RFQ and the SRF-Linac.

We can see that for a given energy, IFMIF-EVEDA has the highest beam power and the highest space charge regime. When considering beam power absolute values, IFMIF-EVEDA can be ranked second. But unlike any other accelerator, even for the most powerful, when the beam power becomes critical from the point of view of losses, let us say for example from 1 MW, IFMIF-EVEDA has by far the highest space charge importance. It means that when the beam power becomes so high that it should be very precisely controlled, because even tiny losses as low as 10^{-6} of the beam must be avoided, the beam behaviour is still very difficult to control due to the importance of space charge effects.

As the space charge effect decreases with energy, particles must be accelerated by the RFQ to energy high enough before being accelerated more efficiently by separated cavities and focusing elements. That is why in IFMIF-EVEDA, the RFQ must accelerate particles to energy as high as 5 MeV, and is the longest RFQ ever constructed.

The space charge effect can also be seen by the tune depression that indicates the focusing deficit experienced by the beam within the periodical structures. Fig. 4 shows that this tune depression in the transverse plane is very low, between 0.4 and 0.6 in the RFQ, and between only 0.2 and 0.4 along the four cryomodules of the SRF-Linac.

3. Challenges and treatment

The unprecedented high beam intensity induces the simultaneous combination of two other unprecedented challenges: high beam power and high space charge. That leads to numerous issues that can be summarised as follows:

- For $E < 5$ MeV, i.e. for the Source Extraction, the LEBT and the RFQ, beam losses are still significant ($\sim$ % of the beam), the issue is to be able to obtain the required 125 mA.
- For $E > 5$ MeV, i.e. for the MEBT, the SRF-Linac and the HEBT, losses induce harmful material activation and must be maintained

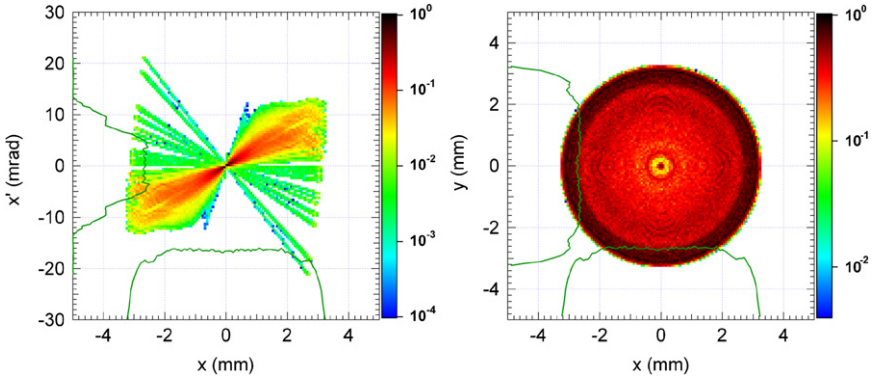

Fig. 5. Beam density distribution at 200 mm from the extraction aperture, in the phase space (left) and the real space (right). In the printed version the densest zone is the darkest one, while in the electronic version black then red are the densest and blue the less dense. (For interpretation of the references to color in this figure legend, the reader is referred to the web version of this article.)

$\ll$ 1 W/m. As simultaneously the beam power is in the MW class, the issue is to avoid micro-losses $\ll 10^{-6}$ of the beam.

These issues, of which a few are conflicting, are furthermore detailed in the following, and the ways foreseen to overcome them are presented.

3.1. Source extraction

In anticipation of possible important losses in the LEBT-RFQ sections, and of the undesirable species extracted, a total extracted current as high as 175 mA is required. Besides, the beam emittance must also be low enough, so that after passing through the LEBT, it must not exceed 0.30 πmm mrad at the RFQ entrance, in order to stay in the range of the RFQ optimum transmission.

Especially at low energy, high current and low emittance are generally conflicting requirements. A higher current means higher space charge forces, contributing strongly to increase the emittance. In order to limit the extracted emittance, it is then necessary to work around effects of space charge forces [1].

Simulations are performed with the codes OPERA2D and AXCEL. Studies use as starting point the extraction system of the SILHI source on the IPHI accelerator, which has proven its excellent performance [2] but intended for lower current and energy. It consists of 5 electrodes with a Φ=9 mm aperture. In a first step, the extraction aperture is considered. As space charge effects are weaker after a bigger waist, the larger the extraction aperture the smaller the beam size and divergence. Considering the beam behaviour for progressively bigger extraction apertures, the aperture diameter Φ=12 mm has been selected, just at the limit of the pumping system. In the second step, the acceleration gap length is progressively reduced, by reducing the number of electrodes. The aim is to move as much as possible the electron repeller toward the plasma electrode, so that the beam reaches as early as possible the area where the space charge is neutralised. If only the beam divergence is considered in configurations with 4 and 3 electrodes, the latter looks the most promising for achieving the smallest extracted beam emittance. However, since the 3-electrode system is less tuneable, the 4-electrode configuration has been selected as a good compromise. Finally, the electrode geometries are finely optimised, in shape and spacing, in order to make them capable of extracting and accelerating the specified beam current while keeping the maximum accelerating field below 100 kV/cm.

In these conditions, the maximum extracted current would be 175 mA, consisting of 140 mA D^+, 26 mA D_2^+, 9 mA D_3^+, according to the standard species composition (respectively, 80%, 15% and 5%). The extracted beam distribution is far from a uniform or a Gaussian distribution, in the phase space as well as in the real one (Fig. 5). In the real space, notice the hollow aspect of the distribution in 2D when looking at the darkest regions in crown form. That is due to the far-from-axis excursion of the highly-divergent beam in the non-linear region of the extraction electrodes, resulting in a folding toward the centre of the beam tail. For the sake of realism, that specific beam distribution will be used as input for all the simulations downstream.

The source and extraction design has been constructed and is being mounted in CEA-Saclay, where tests with beam will be performed, with special attention dedicated to characterising the extracted beam profile. That measured beam profile will then be used as input beam for downstream simulations.

3.2. LEBT

The beam focusing here is made by two solenoids. In this section, the high current implies an important space charge effect, but at this low energy, ionisation cross-section is still large, the D^+ beam will itself sufficiently ionise the residual gas so that released electrons can efficiently compensate its own charge. These competing effects, the space charge and its neutralisation, must be finely studied because the resulting effect along with its detailed location, will significantly affect the beam dynamics.

The SolMaxP code [3] has been used to calculate the resulting radial and longitudinal space-charge potential profile, regarding collision and ionisation mechanisms. With that, it has been demonstrated that the targets are not reached, if all the usual tricks are not employed to enhance the space charge compensation, like additional residual heavy gas (krypton), electron repellers at extraction exit and RFQ entrance. The space charge potential map must also correctly take into account all those equipments as well as the focusing fields. But those calculations are intrinsically very time consuming, of the order of several days on a 50-processor calculator.

In order to limit beam expansion due to space charge, all drifts have been shortened as much as allowed by mechanical design. For example the second solenoid whose focusing is essential for a proper beam injection into the RFQ, is placed the closest to the RFQ entrance, after the numerous equipments as injection cone, electron repeller, pumping ports, cooling system, have been carefully optimised from the mechanical point of view.

The optimisation procedure [4] employs the codes SolMaxP and TraceWin [5]. The optimisation procedure starts with a TraceWin optimisation of the two solenoids fields in the presence of a uniform space charge neutralisation of about 70%. With the two solenoid fields results as input data (as well as the fields of the electron repellers and the extraction system) SolMaxP calculates

the space charge potential map until the steady state is reached. This potential map is then superimposed on the beam line elements and optimisation is performed again with TraceWin in order to recover the best transmission with this new configuration. As the solenoid fields are now slightly changed, the space charge compensation is also modified and another calculation has to be performed again with SolMaxP. Generally, after 2 or 3 steps of such back and forth process, a convergence between the two codes can be reached. The resulting space charge potential map (Fig. 6) is no more uniform, neither radially nor longitudinally. The beam density as well as its total transverse size can be seen in Fig. 7.

This optimisation procedure aims at obtaining the highest beam transmission at the RFQ exit. It is then verified a posteriori that the Twiss parameters at the RFQ entrance are within the theoretical optimum range. This optimisation method was deliberately chosen in order to ensure that it can be reproduced on-line by only looking at the RFQ output current. Indeed, the high compactness dictated by the high space charge regime does not allow implementing more appropriate beam measurements. Furthermore, we have to keep in mind that the real beam output from the ion source could be significantly different from the theoretical one studied here, and that can also change with time, making on-line fine tuning mandatory.

The LEBT line is under construction and will be soon mounted in CEA-Saclay, where consistent tests with beam are planned. Only at the end of those tests the real beam distribution can be known.

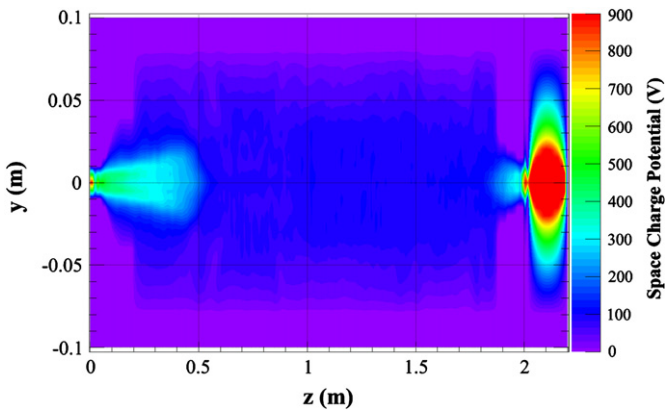

Fig. 6. Final two-dimensional (y,z) space charge potential map. In the printed version the densest zone is the darkest one at the two ends of the graph, while in the electronic version red is the densest and blue the less dense. (For interpretation of the references to color in this figure legend, the reader is referred to the web version of this article.)

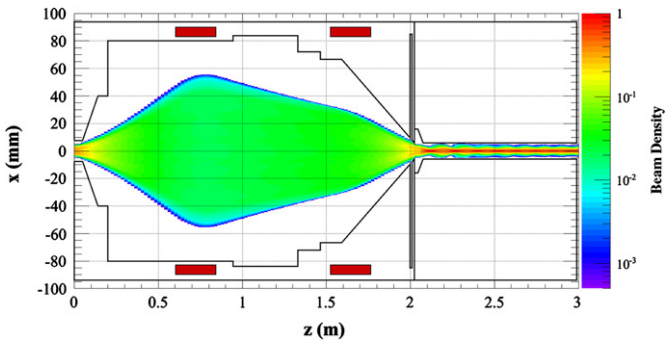

Fig. 7. Beam density along the LEBT and the first RFQ cells. In the printed version the densest zone is the darkest one, while in the electronic version red is the densest and blue the less dense. (For interpretation of the references to color in this figure legend, the reader is referred to the web version of this article.)

3.3. RFQ

First of all, the high space charge regime obliges to accelerate while focusing particles to energy as high as 5 MeV, making the IFMIF-EVEDA RFQ the longest ever constructed. Its length is 9.814 m. A higher energy also means a higher beam power, which is furthermore in an energy range where particle losses begin to induce harmful material activation. Then the bunching task becomes particularly delicate. In addition to facing strong longitudinal space charge, the bunching process must limit as much as possible losses, spread losses on a biggest length in order to lower lost power density, while limiting them to the lower energy part. All that will also induce a longer Gentle Buncher section.

To overcome these difficulties, the RFQ optimisation consists of limiting as far as possible the total length, the losses in high energy part, the maximum surface field, the power consumption [6]. It has been performed with the LANL chain of RFQ codes: Curli→RFQuick→Pari→Parmteqm→Vanes [7]. The focusing strength is chosen to be weak at entrance, $B_0=4$, in order to ease beam injection from the LEBT [8]. Then it grows very fast to $B_0=7$ in order to compensate high space charge forces and to keep the beam in linear force fields. With the same purpose, the design has adopted a "2TERM" geometry type combined with a strong electric focusing to produce extremely linear transverse fields around the beam. At the end of the Gentle Buncher, about the first third of the RFQ, an abrupt decrease of the aperture is intended to loose out-of-energy particles that are not bunched, in order to prevent them from being accelerated to higher energies. On the contrary, in the last third of the RFQ all parameters are left unchanged to avoid losses at energies approaching 5 MeV.

Beam dynamics calculations have been performed using the LANL code PARMTEQM [7] and the CEA code Toutatis [9]. Beam density and losses along the RFQ are displayed in Figs. 8 and 9. Simulations with 10^6 macroparticles show that the ratio of transmitted current reaches 95.9%. The beam not composed of lost particles does not present a significant transverse halo because of the highly focusing nature of a RFQ. It is worth noting that losses are concentrated in the first third part and originate from low energy particles, which are not correctly bunched or accelerated. Locally, the loss power does not exceed 12 W. Only a few particles are lost in the high energy section of the RFQ, but their power can reach 6 W.

A small fraction of the beam (~0.02%) can escape from the RFQ although they are not correctly accelerated. Most of them have an energy around 100 keV and will be therefore lost after the first quadrupole of the MEBT. Only 3 particles out of 10^6 have energies

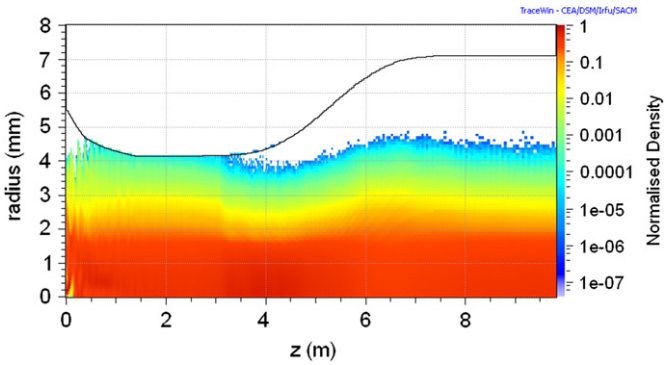

Fig. 8. Beam density along the RFQ. Simulations performed with 10^6 macroparticles. In the printed version the densest zone is the darkest one, while in the electronic version red is the densest and blue the less dense. (For interpretation of the references to color in this figure legend, the reader is referred to the web version of this article.)

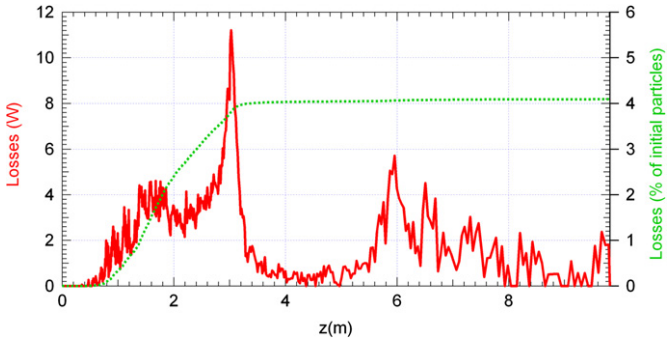

Fig. 9. Beam losses along the RFQ, in beam power (total 1002 W, continuous line and left vertical axis), and in % of initial particles (total 4.1%, dotted line and right vertical axis).

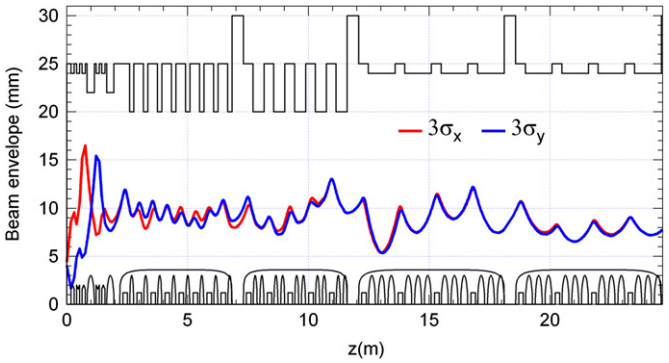

Fig. 10. Beam envelope (3 rms) along the MEBT and the SRF-Linac.

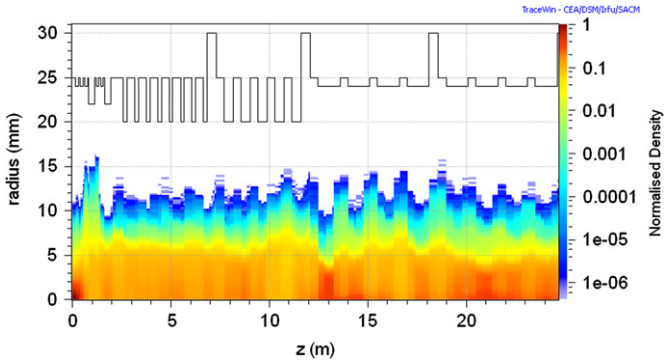

Fig. 11. Beam density along the MEBT and the four cryomodules of the SRF-Linac. Simulation with more than 10^6 macro-particles. In the printed version the densest zone is the darkest one, while in the electronic version red is the densest and blue the less dense. (For interpretation of the references to color in this figure legend, the reader is referred to the web version of this article.)

between 1 and 4.9 MeV. Their loss, much more unpredictable, will occur somewhere downstream, the latest at the HEBT dipole.

The RFQ is under construction at INFN-Legnaro. Tests with beam are planned to be performed after it will be mounted in Rokkasho.

3.4. MEBT and SRF-Linac

The MEBT basic mission would be to transport the 5 MeV beam output from the RFQ and match it for injection into the SRF-Linac. That would mean that the SRF-Linac is a channel with its well defined matched beam in terms of RMS values, to which the input beam just has to be adjusted. Then the tuning of the MEBT and the SRF-Linac are decoupled. The problem is in fact much more delicate.

It appears that RMS quantities are not relevant enough [10], so that the multiparticle aspect must always be considered. Indeed, on one hand, as the beam is space-charge dominated, and as there are long transitions without focusing in the SRF-Linac, any change in the beam distribution will have impact on the net forces acting on the particles, and change their trajectory. On the other hand, as the energy is over 5 MeV, loss-induced material activation becomes harmful and the hands-on maintenance imposes losses to be well less than 1 W/m, which means 10^{-6} of the beam. We call them micro-losses.

All this points out that every simulation or optimisation must be performed for the MEBT and the SRF-Linac together, in multi-particle mode, with at least 10^6 macroparticles, and each macro-particle at the very external beam tail must be carefully examined. This makes optimisations very time consuming.

Furthermore, theoretical calculations have little chance to describe the reality at this degree of precision, as well as it is hard to assure this degree of machine reproducibility. Thus frequent fine tuning is expected in real life, and the numerical optimisation procedure employed to avoid micro-losses must have an on-line equivalent procedure, with the appropriate diagnostics.

To solve this very challenging objective, an uncommon procedure has been adopted. First optimisation is done to match the beam in RMS envelope, then from this starting point, a second optimisation is carried out, aiming at minimising the extent of macroparticles at the external border of the beam. After this step, which is time consuming due to many multiparticle transports, the result is very satisfying: there are no micro-losses, and the beam very external border is regular, far enough from the beam pipe wall. On the contrary, the beam RMS envelope becomes less regular. Everything happens as if a "halo matching" has been performed, instead of the classical "beam matching". We plan to launch calculations with 10^7–10^8 particles to enhance the precision of halo and micro-loss descriptions.

The obtained beam envelope and beam density along the MEBT and the SRF-Linac are shown in Figs. 10 and 11. Assuming that out-of-energy particles from the RFQ have been properly scraped at the MEBT entrance (see Section 5 below), there will be no loss in the superconducting Linac. The halo part, 10^{-5}–10^{-6} at the very external border of the beam, can constitute up to 1/4 of the beam in radius. Its total radius has been especially minimised at the expense of RMS envelope or emittance. As a result, the most external radius of the beam looks more regular than the beam envelope or the core radius (central part in the density graph) and the total emittance growth is 240% in transverse, 160% in longitudinal.

This special behaviour can be understood from the studies of crystalline cold beam [11] showing that, contrarily to homogeneous beam where envelope matching is desirable, for inhomogeneous beam the halo formation can be considerably delayed when the RMS envelope is properly mismatched.

Such a procedure aiming to minimise micro-losses can be used for on-line tunings, on the condition that enough micro-loss detectors can be implemented along the cryomodules, and close enough to the beam pipe, so that the loss distribution can be known with good enough spatial resolution. As the beam size is the biggest in the focusing elements, solenoids in the present case, first micro-losses if any, are expected to happen there. Thus detection of such losses is required at each solenoid.

Besides, it is important to stress that these micro-loss monitors should be used daily for fine tuning, and should be considered as essential as the classical beam position monitors for example. Such a device capable of measuring a fraction of *W* loss is under discussion and not yet decided. Preliminary studies are carried on to measure either the deposited heat, or deposited current, or the

induced neutrons. For the moment, neutron detector by Chemical Vapour Deposition diamond appears to be the most appropriate, and first tests are being performed in CEA-Saclay, France [12].

The EVEDA cryomodule (the first one of IFMIF) is under construction in CEA-Saclay, France.

3.5. HEBT

The EVEDA HEBT has a double mission [13]:

- Transport the 1.1 MW beam and carefully expand it at the beam dump so that the power density does not exceed 300 W/cm^2, and is as symmetrically distributed as possible. Backward radiation from the beam dump is minimised by the 20° dipole.
- Adapt the beam size for beam measurements, in particular for a diagnostic plate of more than 2 m long.

Note that the HEBT is the only section of the accelerator where all the measurements for beam characterisation are planned, which will help to check the validity of beam dynamics calculations under very strong space charge regime, an important step in the validation mission of EVEDA for the final IFMIF.

Seen the beam power, the issues here are to avoid micro-losses while correctly expanding the beam power at the beam dump, as well for nominal conditions as for the different tunings necessary for example for the emittance measurement by quadrupole scanning. Many simulations with 10^6 macroparticles are mandatory, and some of them are not yet finished.

Beam dynamics optimisations have been performed to define magnet locations and beam dump dimensions. In nominal conditions, a beam transport without losses or micro-losses has been obtained (Fig. 12). The input beam is the one coming from the theoretical beam extracted from the ion source. Other beam distributions have been successfully tested, proving the robustness of the HEBT design.

The different magnetic components and the beam dump are being designed and constructed at CIEMAT, Spain.

The IFMIF HEBT has a mission to transport the 5 MW beam toward the liquid lithium target where, with the help of multipolar magnetic elements, it must be expanded in a "perfect" rectangular shape of 5 cm × 20 cm, with a "perfectly" uniform density. For the moment, only preliminary studies have been performed to prove the feasibility of the present HEBT configuration. First section is used to match the beam to the multipole section. It includes two dipoles to minimise backward radiation from the target. The role of the multipoles, two duodecapoles and two octupoles, is to fold the beam tail towards interior in order to obtain a squared beam profile. They are placed at a beam waist in one plane to act on the beam only in the other plane, so that the tunings of the two transverse planes are then roughly uncoupled. The last section allows expanding the beam to the proper size at the target.

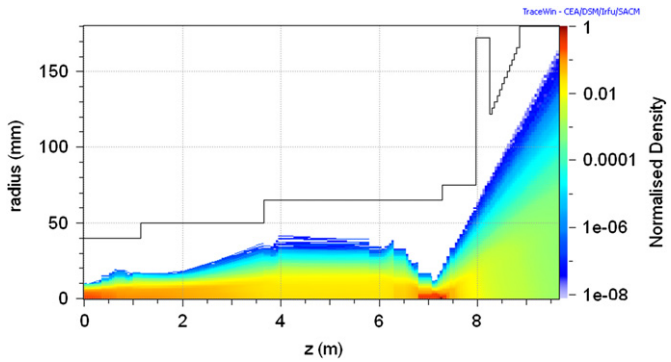

Fig. 12. Beam density along the EVEDA HEBT (prototype accelerator) that drives the beam against the beam dump. In the printed version the densest zone is the darkest one, while in the electronic version red is the densest and blue the less dense. (For interpretation of the references to color in this figure legend, the reader is referred to the web version of this article.)

Actually, with space charge forces, the beam waists cannot be perfect and the transverse planes are not uncoupled any more. Furthermore, the multipole magnets introduce themselves changes on the downstream waists. To achieve the ideal beam footprint requires a long and complex process involving all the magnetic elements. A more systematic method or a clearer tuning strategy remains to be found.

Besides, seen the beam power of 2 × 5 MW, any small deviation from the ideal situation could consistently bias results of physics experiments or strongly damage equipments. Many more studies remain to be performed in order to estimate the reliability, the reproducibility and the stability of such a beam.

4. Error studies and loss catalogue

The results shown above are obtained in the nominal case without any error on the beam input nor on the structure. In our case, the importance of error considerations is further crucial for studying the sensitivity to errors of the very external particles of the halo, which can lead to microlosses. Up to now, error studies have been performed separately for each of the above described section of the accelerator. It has been carried out following several steps:

- First of all, each type of error (mechanical alignment or field strength) is switched on individually to characterise its effect on the trajectory and the resulting beam steerers, as well as on the beam envelope, emittance and halo. For the EVEDA HEBT, the beam density variation at the beam dump is also carefully considered.
- Then relative strengths are distributed to every error so that they all individually lead to about the same effects.
- Finally a same coefficient is applied to all the errors, which is progressively increased up to a threshold where their effects can be judged as still acceptable. Tolerances and steerer strengths are determined in this way.

Static and dynamic errors have been considered: the former allow trajectory correction whereas the latter are so fast that no correction can be applied. Simulations show that for conservative tolerances, combined static and dynamic errors do not lead to significant increase in halo or microlosses.

In the near future, start-to-end simulations with errors in the structure and in the initial beam input remain to be carried out.

Besides, due to the very high power of the beam, any loss, even tiny, can be harmful. Careful and detailed loss studies remain to be performed in the following three situations: nominal situations, tuning situations and accidental situations. Such a catalogue will be useful, or even necessary in the definition of safety procedures, limitations and recommendations, aiming at protecting personnel and equipments. A protocol has been established for these studies:

- Nominal situations. "Nominal" means here ideal theoretical conditions, without any error. That should correspond on the real machine, to a completely satisfying situation, once the beam has been perfectly corrected and perfectly tuned. Losses in such conditions will be minimal, we cannot hope to have less. These are minimum and permanent losses we will have to withstand. This concerns all the nominal settings,

including those applied during beam commissioning, which are different.

- Tuning situations. It consists of estimating losses that can occur before or during tuning and correction procedures, necessary for obtaining a satisfactory operation of the accelerator. These losses, larger than the nominal ones, are due to all the possible differences between the ideal, theoretical machine and the real one. These differences can be divided into two categories: the components that do not respect exactly the theoretical specifications or the beam behaviour is not exactly the same than what is theoretically simulated (think of the IFMIF very high space charge regime that has never been implemented). These situations can be taken into account by simulating 1000 machines with suitable "errors", without any corrector. The "errors" should be of two kinds: mechanical and alignment errors, randomly distributed within the already determined tolerances, and tuneable parameters (gradient, field, phase, RF power, pressure, etc.), randomly distributed within a range that can be estimated as likely on the real machine, for example $\pm 10\%$ of the nominal values.
- Accidental situations. These situations are not the same for all the sections. Reflexions and analysis should be carried out to detect which is the worst case, which is the main affected location or equipment, when one tuneable parameter (gradient, field, phase, RF power, pressure, etc.), or a given combination of them, are suddenly switched off. But attention will also be paid to detect if there is an intermediate case, which can induce more losses, for example in the transition from the nominal value to zero for specific field or gradient. Situations where correctors or BPMs suddenly fail are also to be considered. These studies are hard to be exhaustive. The objective would be just trying to point out for each section the worst cases where the beam could hit equipment with the highest power density.

5. Beam collimation

For a high power accelerator such as IFMIF, despite its necessary compactness inducing space shortage, collimation systems have been foreseen in the LEBT, MEBT and HEBT in order to, respectively, protect the RFQ, the SRF-Linac and the beam dump.

At the end of the LEBT, an injection cone prevents the RFQ entrance from being hit by out-of-emittance particles coming from the injected beam, especially the undesirable ion species D_2^+, D_3^+ that are naturally not focused enough compared to the nominal D^+ ions. This cone is designed to withstand 5 kW of beam heating.

Always in the LEBT, a chopper is foreseen between the two solenoids, consisting of two plates of 150 mm length where a 4 kV potential difference can be applied. IFMIF is designed to be operated in CW mode, but it is planned to perform beam measurements with interceptive diagnostics during the first beam commissioning stage at low duty cycle. Even at the lowest duty cycle, 10^{-3}, the average beam power at RFQ exit is still 600 W at 600 MeV, and the deposited energy is hard to be withstood by diagnostics like grids or slits. The chopper will allow lowering the duty cycle down to 10^{-4}. Another advantage is to provide 100 μs pulses of beam close to its nominal condition because the first rising part of the pulse delivered by the ion source can be cut off.

Further in the accelerator, appropriate scrapers must be installed in the MEBT to preserve the superconducting Linac from halo particles coming from the RFQ. An efficient collimation scheme would use pairs of scrapers, 90° phase advance apart. Unfortunately, as the MEBT length is very short, this scraper configuration is not possible. The method instead consists of distinguishing the two different undesirable particle types that must be stopped: out-of-energy particles that have not been correctly accelerated through the RFQ and out-of-emittance particles contained in the transverse beam halo. The former, at lower energies than the nominal energy, are already partly lost in the very first part of the MEBT and will be more scattered after the first defocusing quadrupole. They have to be stopped there. The latter have to be stopped where the beam size is the biggest. A pair of scrapers have been recommended, a first vertical one just downstream the first quadrupole that is defocusing in vertical, and a second horizontal one downstream the second quadrupole where the beam is the biggest in horizontal. The efficiency of such scrapers has been extensively checked with various simulated beam distributions coming from the RFQ, where the halo part has been artificially enhanced consistently to improve the statistic. As the ideal scraping aperture depends on the halo distribution, and as the scraping efficiency varies exponentially with that aperture, movable scrapers are strongly recommended.

At the end of the IFMIF prototype accelerator, the beam dump in cone shape is designed with appropriate geometry and cooling for absorbing the whole beam power of 1.1 MW, at the condition that the beam is injected correctly into the foreseen aperture. If for any reason there is substantial power deposition on the surrounding area of the beam dump entrance, for example the bellow in front of it, the induced damage cannot be easily repaired because it is located in a highly radioactive zone. That is why, a scraper is also foreseen at the end of the HEBT in order to limit the impact of particles in the beam halo on to the perimeter of the beam dump entrance.

6. A "laboratory" for high intensity beam studies

The above described procedures allow finding out immediate beam dynamics solutions for the challenging IFMIF objectives, but much remains to be done in order to well understand the physics of its very high intensity beam. It has been observed for example that once the external beam limit is perfectly minimised and regular along the SRF-Linac, the emittance can sometimes literally blow up. A compromise is often necessary between halo and emittance minimisations.

In Ref. [14], the reason of emittance growth has been sought by looking at the two competing terms of the envelope equations, the emittance term and the space charge term [15], which are given by

$$E_{x,y} = \frac{\varepsilon_{x,y}^2}{\sigma_{x,y}^3} \tag{2}$$

$$SC = \frac{K}{2(\sigma_x + \sigma_y)} \tag{3}$$

where $\varepsilon_{x,y}$ is the horizontal, vertical non-normalised emittance, $\sigma_{x,y}$ is the corresponding RMS beam size and K the generalised perveance. But this SC term, although valid for all types of distribution with elliptical symmetry, is rather valid for a continuous beam. In case of bunched beams, it is more correct to use instead

$$SC_3 = \frac{3K_3(1-f)}{(\sigma_x + \sigma_y)\sigma_z} \tag{4}$$

where f is an ellipsoid form factor from Ref. [16], and K_3 the 3-D space-charge parameter in Ref. [15]. The problem is that K_3 depends on a coefficient that varies with the particle distribution type. To choose the appropriate coefficient corresponding to our case, we can remark that when the longitudinal dimension is

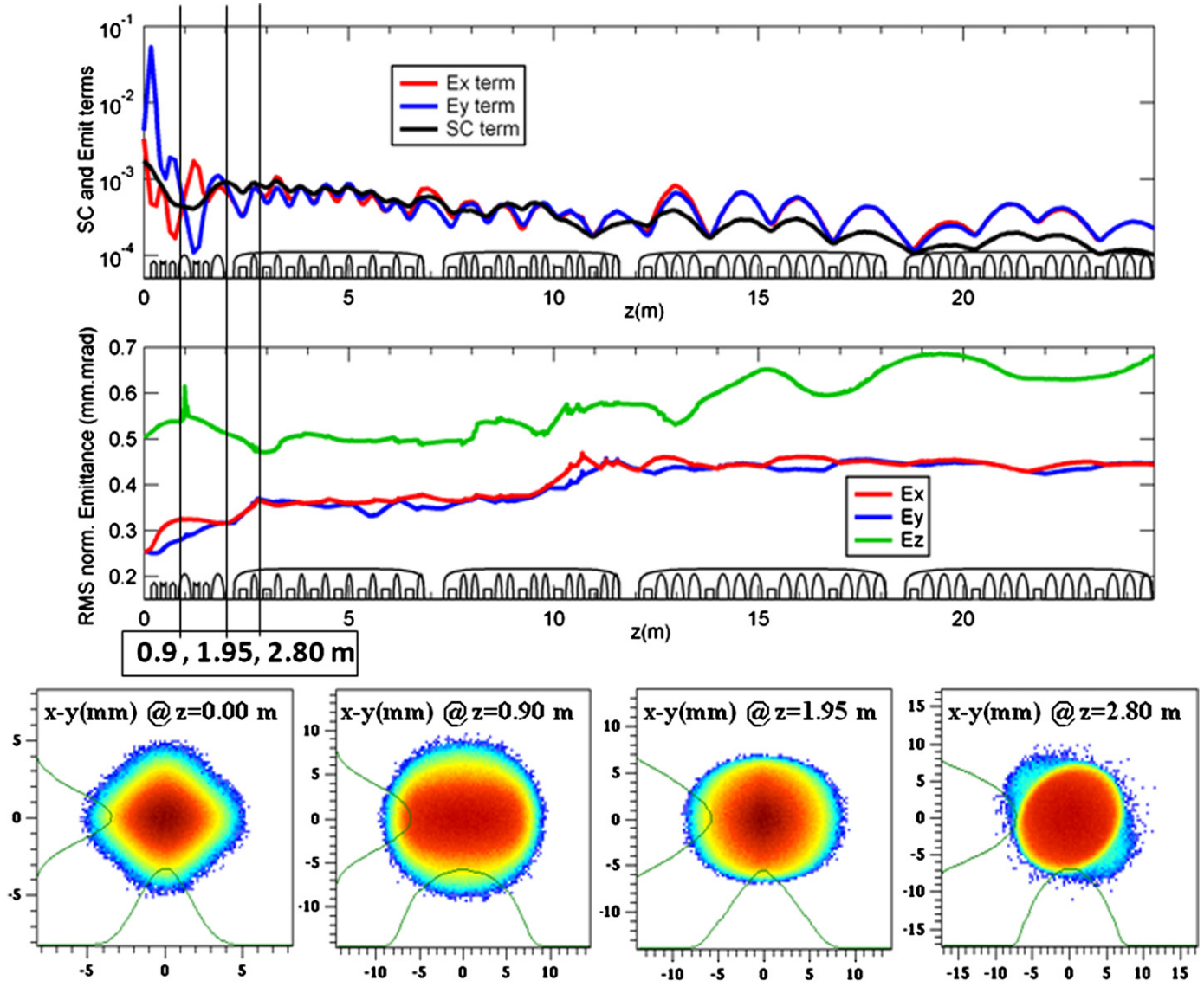

Fig. 13. Variation of $E_{x,y}$ and SC_3 terms along the MEBT and the four cryomodules of the SRF-Linac (top). The corresponding variation of emittance is also given (centre). The beam presents remarkable behaviours (see text) at the positions $z=0.90$, 1.95, 2.80 m. Beam density in the x–y space, and its projection in x and y, are given for $z=0$ and these positions (bottom). In the printed version the densest zone is the darkest one toward the centre, while in the electronic version red is the densest and blue the less dense. The density projection in x and y are represented by the continuous thin line, which is green in the electronic version. (For interpretation of the references to color in this figure legend, the reader is referred to the web version of this article.)

much greater than the transversal ones, $f\rightarrow 0$ and $SC_3=SC$. As at one location very close to the RFQ exit, the beam is in such a condition ($f \lesssim 0.1$), we can find out the coefficient in the K_3 expression by equalising SC_3 and SC there.

The comparative evolution of SC_3 and $E_{x,y}$ is given in Fig. 13 along with the MEBT and the four cryomodules of the SRF-Linac. The corresponding emittance growth is also given in the same figure.

After careful examination, the first emittance growths till the SRF-Linac entrance look understandable. Whenever the SC term is larger than the E_x or E_y term, meaning that the beam is space charge dominant, the emittance grows in the corresponding plane. Right at the RFQ exit ($z=0$ m), $SC_3 > E_x$, the horizontal emittance immediately grows, up to $z\sim 0.9$ m where the situation is inversed. In the vertical plane, E_y is larger than SC_3 at $z=0$ m, then progressively decreases below at $z\sim 0.9$ m, that is why the vertical emittance grows after and slower than the horizontal one and continues to grow after 0.9 m, up to about $z=1.90$ m. But then, close to the MEBT end at $z\sim 1.95$ m where the beam begins to get cylindrically symmetric, it is again in the condition where the horizontal and vertical emittances grow together up to $z\sim 2.80$ m, where an equilibrium is reached.

We can see at each time that the growing distance is about 0.90 m, which corresponds to the average length covered by the beam during a quarter of the plasma oscillating time, given by

$$\tau_{plasma} = 2\pi\sqrt{\epsilon_0 m_0/nq^2}, \tag{5}$$

n being the beam density. This is typical of the classical mechanism of charge redistribution when the beam leaves a strong focusing environment for a less strong one. Here, the first time is the transition from the RFQ to the MEBT, and the second one is due to the long transition without transverse focusing between the last MEBT quadrupole and the first cryomodule solenoid.

This mechanism can also be clearly seen in the x–y beam density (Fig. 13, bottom) when looking at the importance of the maximum density (red area), or the projections in x and y (green line). For x and y, at $z=0$ m, as well as for only x, at

$z=1.95$ m, the beam has a large tail, typical of a space charge dominated beam, leading to emittance growth. On the contrary, for x and to a less extent for y, at $z=0.9$ m, then for x and y, at $z=2.8$ m, the beam has a much more compact profile, due to rapid charge redistribution to provide shielding to the external focusing field. This is typical of an emittance dominated beam, stopping the emittance growth process.

However, the emittance growths in the next sections as well as in longitudinal does not present such behaviours and thus cannot be explained by that mechanism. Resonance and/or coupling mechanisms should rather be invoked. Additional exciting studies should be carried out in order to better understand the processes leading to emittance and/or halo growths. From this point of view, we are in the presence of a true "laboratory" for High Intensity Beam studies.

7. Conclusion

The IFMIF-EVEDA record intensity, which induces simultaneously the highest beam power, the highest space charge and the longest RFQ, requires that unprecedented challenges have to be faced in beam dynamics design and optimisation. For this Megawatt-class accelerator, new concepts have emerged: micro-losses, halo matching, essential diagnostics. Indeed, special attention must be paid to manage tiny losses well lower than 10^{-6}, so that usual methods as beam matching are no more relevant, halo matching should be performed instead, to take care of the edge of the beam tail. As simulations are not expected to reach this degree of precision and equipments to reach this degree of reproducibility, theoretical beam dynamics tuning must have its equivalence for on-line fine tuning. Special diagnostics are then required, considered as essential diagnostics, i.e. essential for reaching the targeted performances.

And the most important is that such Megawatt-class accelerators provide a tremendous opportunity for studying High Intensity Beam Physics in its most extreme limit.

References

[1] O. Delferrière, et al., in: Proceedings of ICIS 2007, Jeju, Korea, 2007.
[2] R. Gobin, et al., Rev. Sci. Instrum. 73 (2) (2002) 922.
[3] R. Duperrier, D. Uriot, IFMIF Report, CEA, 2008.
[4] N. Chauvin, et al., in: Proceedings of PAC 2009, TH5PFP004, Vancouver, Canada, 2009.
[5] R. Duperrier, N. Pichoff, D. Uriot, in: Proceedings of ICCS 2002, Amsterdam, Netherlands, 2002.
[6] M. Comunian, in: Proceedings of LINAC 2008, MOP036, Victoria, Canada, 2008.
[7] K.R..Crandall, T.P. Wangler, Los Alamos National Laboratory Report, LA-UR-88-1546, 1987.
[8] L.M. Young, in: Proceedings of PAC 2001, WOAA004, Chicago, USA, 2001.
[9] R. Duperrier, Phys. Rev. 3 (2000) 124201.
[10] N. Chauvin, et al., Proceedings of PAC 2009, TH5PFP005, Vancouver, Canada, 2009.
[11] E.G. Souza, et al., Appl. Phys. Lett. 96 (2010) 141503.
[12] J. Marroncle, et al., in: Proceedings of DIPAC 2011, Hamburg, Germany, in preparation.
[13] C. Oliver, et al., in: Proceedings of EPAC 2008, THPC028, Genoa, Italy, 2008.
[14] P.A.P. Nghiem, et al., in: Proceedings of PAC 2009, TH5PFP006, Vancouver, Canada, 2009.
[15] T.P. Wangler, RF Linear Accelerators, Wiley-VCH, 2008, p. 298.
[16] P. Lapostolle, CERN Report AR/INT SG/65-15, 1965.